

The 18 May 2024 superbolide over the Iberian Peninsula: USG space sensors and ground-based independent observations

E. Peña-Asensio,^{1,2*} P. Grèbol-Tomàs,^{2,3} J. M. Trigo-Rodríguez,^{2,3} P. Ramírez-Moreta,⁴ and R. Kresken⁴

¹Department of Aerospace Science and Technology, Politecnico di Milano, Via La Masa 34, 20156 Milano, Italy

²Institut de Ciències de l'Espai (ICE, CSIC) Campus UAB, C/ de Can Magrans s/n, 08193 Cerdanyola del Vallès, Catalonia, Spain

³Institut d'Estudis Espacials de Catalunya (IEEC) 08034 Barcelona, Catalonia, Spain

⁴ESA/ESAC/Planetary Defence Office (OPS-SP) Camino Bajo del Castillo s/n, 28692 Villanueva de la Cañada, Madrid, Spain

Accepted XXX. Received YYY; in original form May 23, 2024

ABSTRACT

On 18 May 2024, a superbolide traversed the western part of the Iberian Peninsula, culminating its flight over the Atlantic Ocean and generating significant media attention. This event was caused by a weak carbonaceous meteoroid of 89.8 ± 0.4 cm, with a density of 1660 kg m^{-3} , entering the atmosphere at 41.6 km s^{-1} with an angle of 10.9° . The luminous phase started at 138 km and ended at an altitude of 54 km. The meteoroid's heliocentric orbit was characterized by an inclination of 15.4° , a high eccentricity of 0.965, a semi-major axis of 3 au, and a notably short perihelion distance of 0.11 au. The superbolide was recorded by multiple ground-based stations of the Spanish Meteor Network (SPMN), the European Space Agency (ESA), and the U.S. Government (USG) space sensors. Our analysis shows a relatively good agreement with the radiant and velocity data reported by the Center for Near-Earth Object Studies (CNEOS), with a deviation of 1° and 1.2 km s^{-1} , respectively. Due to the absence of observable deceleration, we successfully reconciled satellite radiometric data with a purely dynamic atmospheric flight model, constraining the meteoroid's mass and coherently fitting its velocity profile. The inferred bulk density and aerodynamic strength of the meteoroid from the flight model are compatible with the properties recently measured for sample-returned materials from asteroid Bennu. The physical properties and the orbital results suggest that this meteoroid originated from a recent disruption of a comet, indicating the existence of hazardous meter-sized projectiles arriving on Earth from objects formed in the distant regions of the Solar System.

Key words: Superbolide – Fireball Network – Space Sensors – Atmospheric Flight – Orbit

1 INTRODUCTION

On 18 May 2024, an exceptionally luminous fireball was observed over Spain and Portugal. This event was captured on video by casual observers and quickly disseminated through the media. Additionally, it was recorded by various wide-field and multi-camera stations that continuously monitor the sky over the Iberian Peninsula. The U.S. Government (USG) space sensors also detected the event, as reported on the Center for Near-Earth Object Studies (CNEOS) fireball website¹. Following confirmation of its detection from space², the event can be formally classified as a superbolide (Ceplecha et al. 1999). These exceptionally bright fireballs are produced by the hypersonic atmospheric entry of meter-sized natural projectiles (Ceplecha et al. 1998; Silber et al. 2018). The study of superbolides provides valuable insights into the physical properties, dynamics, and impact hazard issues associated with the near-Earth asteroid population (Koschny & Borovicka 2017; Trigo-Rodríguez 2022).

The CNEOS catalog, managed by NASA's Jet Propulsion Laboratory, archives data on fireball events detected via various USG satellite sensors (Tagliaferri et al. 1994). Superbolides are relatively rare events that can occur over remote areas. USG sensors provide near-global coverage of large meteoroids and small asteroids impacting the Earth's atmosphere, unlike the ground-based meteor network which only monitors a relatively small, fixed atmospheric volume. Therefore, the CNEOS catalog is of scientific interest as it extends the projectile flux estimations by utilizing the entire planet as a detector, capturing events that are typically singular occurrences for other techniques (Brown et al. 2002).

As of May 2024, the catalog contains 979 fireball events, with velocity vector and altitude data available for 310 cases. For these events, detailed information is provided, including geographic coordinates, terminal disruption altitude, vector velocity components in an Earth-Centered, Earth-Fixed (ECEF) reference frame, and estimated radiated and impact energies. These energies, linked by an empirical formula, are among the most reliable parameters provided by CNEOS (Brown et al. 2002).

However, specific information about these sensors remains undisclosed, as they are classified data. In any case, we previously prepared our *3D-FireTOC* software to compute future detections based on CNEOS-released data (Peña-Asensio et al. 2021b) and performed

* E-mail: eloy.pena@polimi.it, eloy.peas@gmail.com

¹ <https://cneos.jpl.nasa.gov/>

² It was also detected by ESA's Meteosat 3Gen (MTG) satellite via its Lightning Imager instrument: https://www.esa.int/Applications/Observing_the_Earth/Meteorological_missions/meteosat_third_generation/Fireball_witnessed_by_weather_satellite

Table 1. Longitude, latitude, and altitude of the 4 selected stations recording the SPMN180524F superbolide.

| Station | Lon. (°) | Lat. (°) | Alt. (m) |
|-----------------------|----------------|-----------------|----------|
| Navianos de Valverde | 5° 48' 48.4" W | 41° 57' 11.6" N | 711 |
| Estepa | 4° 52' 35.6" W | 37° 17' 29" N | 537 |
| Sanlúcar de Barrameda | 6° 20' 31" W | 36° 46' 30.3" N | 6 |
| Casas de Millán | 6° 19' 57.8" W | 39° 51' 4.8" N | 739 |

an analysis of the CNEOS catalog (Peña-Asensio et al. 2022). The accuracy of the CNEOS data has been assessed through comparisons with ground-based observations of fireballs (Devillepoix et al. 2019; Peña-Asensio et al. 2022; Brown & Borovička 2023; Peña-Asensio et al. 2024). To date, only 17 fireballs in the CNEOS catalog have been benchmarked with independent counterparts. Here we report and compare a new event detected by the USG space sensors and multiple ground-based fireball networks.

2 OBSERVATIONS AND METHODS

2.1 Ground-based observation

On the night of Saturday, May 18, 2024, a remarkable superbolide was observed over the Iberian Peninsula at 22:46:49 UTC, specifically flying over Extremadura and northern Portugal, before its trajectory concluded over the Atlantic Ocean. It was recorded by the Spanish Fireball and Meteorite Network (SPMN) (Trigo-Rodríguez et al. 2004), as well as by AMS82, one of the European Space Agency's (ESA) Planetary Defense Office meteor stations of the AllSky7 Network³, located in Casas de Millán, Cáceres, Spain. Designated as SPMN180524F by the SPMN network, this event was notable for its intense brightness which momentarily turned night into day, causing a massive media impact. The superbolide exhibited an atmospherically originated bluish-green glow and left a persistent luminous trail in the sky. Table 1 lists the stations used in this study, while Figure 1 shows the max-combined video frames as observed from each station.

Many casual videos immediately surfaced in the media, underscoring the importance of promptly explaining these unusual phenomena to the public. Some of the videos are particularly extraordinary, as the bolide was captured from a relatively close distance, revealing significant variations in brightness along its extensive luminous trajectory. These fluctuations in luminosity are typically associated with the continuous fragmentation of the meteoroid and the release of dust and fragments ablated by the heat generated in the frontal shock wave, a characteristic behavior of impacting crumbly meteoroids (Revelle 2002).

We use our *3D-FireTOC* software to analyze the event. This tool integrates computer vision and machine learning for detecting and tracking fireballs, robust camera calibration to correct distortions, the plane intersection method for triangulation, and heliocentric orbit determination (Peña-Asensio et al. 2021b,a, 2023b,a). Using a model of atmospheric mass density and the measured velocity, the dynamic strength where the meteoroid disruption occurs is computed as $S = \rho_{atm} v^2$ (Bronshten 1983). From that, thanks to the empirical strength-density relation established by Collins et al. (2005), we calculate the impactor density as:

$$\rho_m = \left(\frac{\log_{10} S - 2.107}{0.0624} \right)^2. \quad (1)$$

At the onset of the luminous phase and down to altitudes near 60 km, the atmosphere is sufficiently thin that deceleration is barely observable. Consequently, all measured points during this phase equally represent the initial velocity, allowing for a robust estimate.

2.2 Space-based observation

From the perspective of the CNEOS catalog, the SPMN180524F superbolide, with a total impact energy of 0.13 kt, is not a common event: it holds the highest height in the database, ranks as the fifth fastest with respect to the Earth, and is the fourth with the lowest density (see Fig. 2). The density estimation process is the same as described in the previous section.

As the superbolide did not penetrate deeply into the atmosphere and was observed from long distances, the ground-based measurements are insufficient for fitting a dynamic deceleration model. Therefore, we use as a proxy the total radiated energy (E) measured by the USG sensors, which has proven reliable. By assuming that the energy recorded is equal to the kinetic energy, we estimate the initial mass of the projectile as:

$$m_0 = \frac{2E}{v^2}. \quad (2)$$

By leveraging the dynamic, dimensionless approach based on the single body theory, the so-called α - β method (ballistic coefficient and mass-loss parameter, respectively), we can characterize the atmospheric flight by reverting Eq. 14 of Gritsevich (2009):

$$\alpha = \frac{c_d \rho_0 h_0 A}{2m_0^{1/3} \rho_m^{2/3} \sin \gamma}, \quad (3)$$

where $c_d = 0.7$ is the drag coefficient, $A = 1.21$ is the spherical shape factor, $\rho_0 = 1.29 \text{ kg m}^{-3}$ is the atmospheric density at the sea level, $h_0 = 7.16 \text{ km}$ is the height of the homogeneous atmosphere, and γ is the slope of the trajectory from the horizon.

By assuming the terminal mass is equal to zero, β can be estimated from the terminal height h_e and α (Moreno-Ibáñez et al. 2015):

$$\beta = \frac{e^{h_e/h_0}}{2\alpha}. \quad (4)$$

With α and β determined, we fit the atmospheric flight model to the observed data to obtain the velocity profile (Gritsevich 2007):

$$h(v) = \ln 2\alpha + \beta - \ln(\overline{Ei}(\beta) - \overline{Ei}(\beta v^2)), \quad (5)$$

where

$$\overline{Ei}(x) = \int_{-\infty}^x \frac{e^z dz}{z}.$$

3 RESULTS AND COMPARISON

Figure 3 displays the 3D reconstruction of the atmospheric flight, and Figure 4 depicts its characterization. The heliocentric orbits derived from the ground-based observations and the space sensors are illustrated in Figure 5. Table 2 shows all parameters derived from the ground- and space-based observations.

³ www.allsky7.com

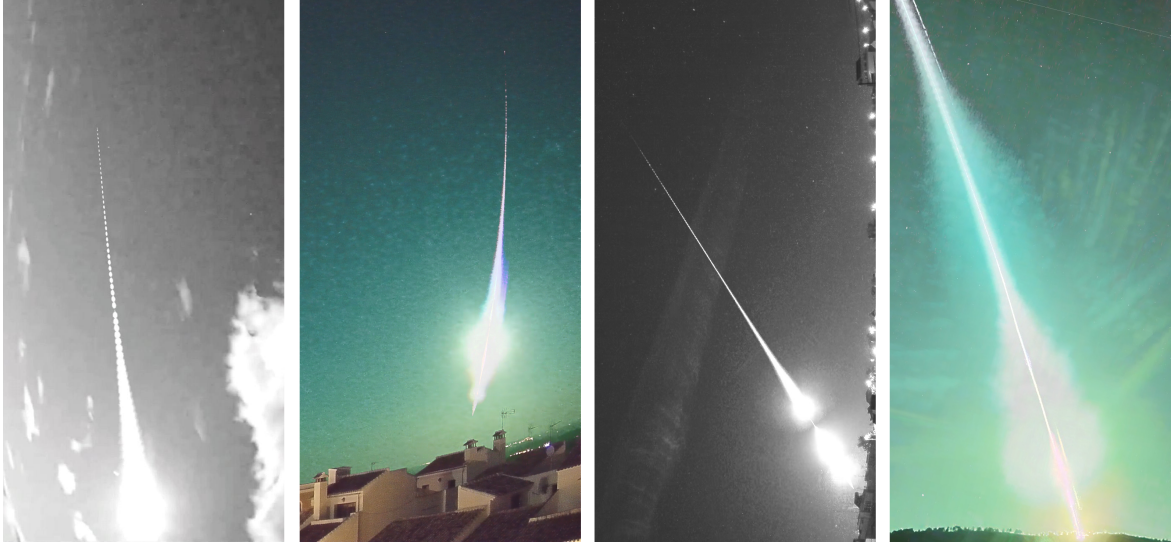


Figure 1. The four videos used in this work to study the superbolide SPMN180524F. The images are max-combined from the video frames. Some saturated frames have been removed for illustration purposes. From left to right: Navianos de Valverde, Estepa, Sanlúcar de Barrameda, and Casas de Millán.

Table 2. Atmospheric flight, physical parameters, and osculating heliocentric orbital elements of the SPMN180524F superbolide.

| Parameter | | Ground-based | CNEOS | Discrepancy |
|--|-------------|---------------------|---------------------|-------------|
| Initial time [UTC] | t_0 | 2024-05-18 22:46:42 | | |
| Initial longitude [°] | λ_0 | 5.5197±0.0010 W | | |
| Initial latitude [°] | φ_0 | 38.5777±0.0011 N | | |
| Initial velocity [km s ⁻¹] | v_0 | 41.64±0.19 | | |
| Initial height [km] | h_0 | 137.88±0.05 | | |
| Final time [UTC] | t_e | 2024-05-18 22:46:53 | | |
| Final longitude [°] | λ_e | 9.885±0.005 W | | |
| Final latitude [°] | φ_e | 42.112±0.005 N | | |
| Final velocity [km s ⁻¹] | v_e | 40.03±0.17 | | |
| Final height [km] | h_e | 53.78±0.07 | | |
| Energy peak time [UTC] | t_p | 2024-05-18 22:46:49 | 2024-05-18 22:46:50 | -1 s |
| Energy peak longitude [°] | λ_p | 8.2932±0.0017 W | 8.8 W | -0.5068 |
| Energy peak latitude [°] | φ_p | 40.8851±0.0015 N | 41.0 N | -0.1149 |
| Energy peak velocity [km s ⁻¹] | v_p | 41.63±0.19 | 40.4 | 1.23 |
| Energy peak height [km] | h_p | 77.91±0.04 | 74.3 | 3.61 |
| Length [km] | Δl | 554.2±0.4 | | |
| Slope [°] | γ | 10.93±0.02 | 6.5 | 4.43 |
| Azimuth [°] | A | 317.75±0.04 | 315.8 | 1.95 |
| Dynamic strength [kPa] | S | 44.4±0.4 | 72.41 | -28.01 |
| Meteoroid density [kg m ⁻³] | ρ_m | 1658±6 | 1946 | -288 |
| Meteoroid mass [kg] | m_0 | 628±6 | 666 | -38 |
| Initial diameter [cm] | D | 89.8±0.4 | 87 | 2.8 |
| Geo. velocity [km s ⁻¹] | v_R | 39.87±0.19 | 38.6 | 1.27 |
| Geo. radiant R.A. [°] | α_R | 261.56±0.04 | 262.4 | -0.84 |
| Geo. radiant Dec. [°] | δ_R | -28.13±0.04 | -29.7 | 1.57 |
| Semi-major axis [au] | a | 3.01±0.11 | 2.3 | 0.71 |
| Eccentricity | e | 0.965±0.002 | 0.95 | 0.015 |
| Inclination [°] | i | 15.39±0.12 | 18.2 | -2.81 |
| Argument of periapsis [°] | ω | 145.52±0.12 | 145.4 | 0.12 |
| Long. of the asc. node [°] | Ω | 238.1257±0.0001 | 238.1321 | -0.0064 |
| Perihelion distance [au] | q | 0.106±0.001 | 0.11 | -0.004 |
| True anomaly [°] | f | 214.49±0.12 | 214.6 | -0.11 |
| Period [year] | P | 5.2±0.3 | 3.5 | 1.7 |
| Tisserand's parameter | T_j | 2.1±0.1 | 2.7 | -0.6 |
| Ballistic coefficient | α | 17.22±0.05 | | |
| Mass-loss parameter | β | 53.1±0.4 | | |

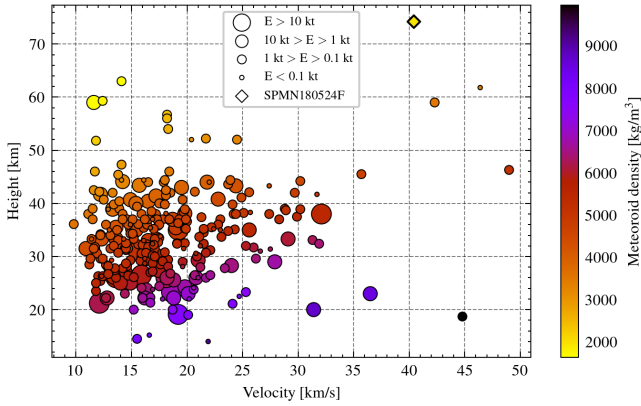


Figure 2. CNEOS fireballs with sufficient data (velocity and height at the peak of radiated energy) to estimate the projectile density.

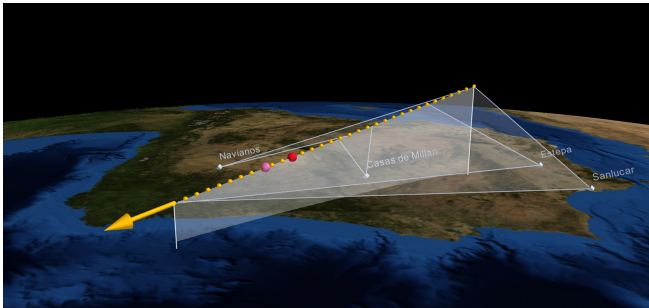


Figure 3. Atmospheric flight of the superbolide SPMN180524F. For ground-based observations, the peak brightness occurs at the red point. In pink is shown the point reported by the USG space sensors.

The search for possible associations with meteoroid streams or parent bodies for superbolide SPMN180524F yielded negative results using both traditional D-criteria and Machine Learning distance metrics (Peña-Asensio & Sánchez-Lozano 2024). If the SPMN180524F superbolide resulted from a cometary disruption, additional fragments could potentially reach the Earth. Nevertheless, these are difficult to detect in advance due to the typical low albedo of carbonaceous chondrites (Trigo-Rodríguez et al. 2014; Tanbakouei et al. 2020). Given the estimated meteoroid size of approximately 0.9 m and a density of 1660 kg m^{-3} , we hypothesize its origin might be the disruption of a comet. Remarkably, a recent study of the samples returned by the OSIRIS-REx NASA mission revealed similar bulk density values (Lauretta et al. 2024), which could suggest a Bennu-like parent body.

The scenario of SPMN180524F originating from a disrupted comet is plausible, as its orbital eccentricity carried the meteoroid well beyond the orbit of Jupiter. The plausible connection between carbonaceous chondrites (CCs) and comets, long suggested, is further supported by recent studies of the reflectance spectra of comet 2P/Encke and ungrouped CCs (Tanbakouei et al. 2020). The role of erosion and subsequent dehydration caused by thermal processing of cometary nuclei was elucidated by Rosetta’s study of 67P/Churyumov-Gerasimenko, providing insights into the evolution of meteoroids resulting from their disruption (Fulle et al. 2020; Koschny et al. 2019; Trigo-Rodríguez et al. 2019). Researches on cometary formation and disintegration products suggest that

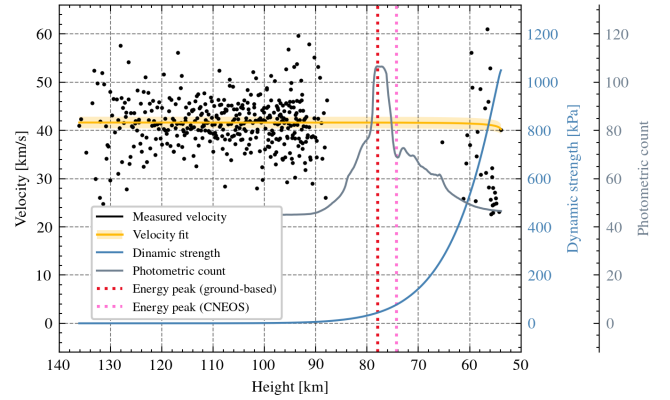


Figure 4. Characterization of the atmospheric flight of the superbolide SPMN180524F. It includes the measured velocity points, the best fit for the velocity with $3\text{-}\sigma$ uncertainty, the dynamic strength, and the uncalibrated photometric counts from Estepa.

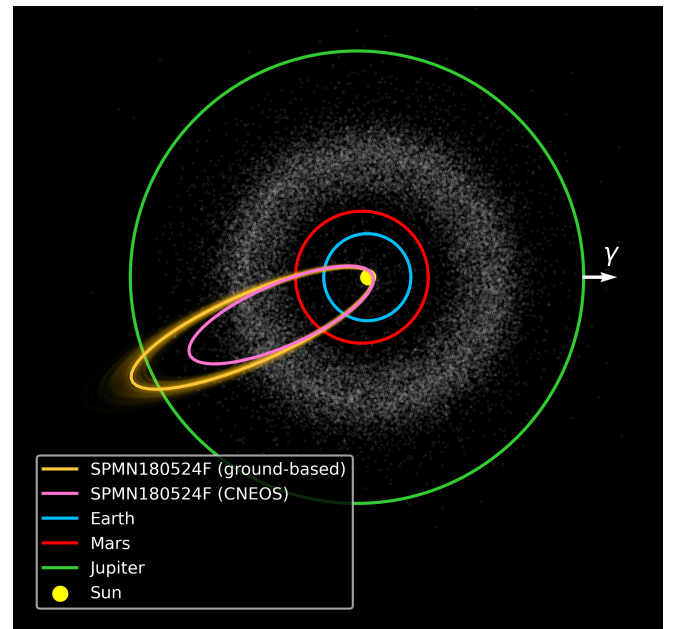


Figure 5. Osculating heliocentric orbit of the superbolide SPMN180524F determined from ground and space observations.

centimeter-sized pebbles with higher density can be preserved in the interior of comets (Schräpler et al. 2022; Trigo-Rodríguez & Blum 2022). These pebbles can survive at higher dynamic strengths than the fine-grained materials forming the meteoroid interstitial matrix.

There are examples of superbolides produced by carbonaceous chondrite (CC) projectiles, such as the Tagish Lake meteorite fall, which had an estimated meteoroid density of 1500 kg m^{-3} but resulted in higher density ungrouped CCs (Brown et al. 2000), as well as the Maribo, Sutter’s Mill, Flensburg, and Winchcombe meteorites (Haack et al. 2012; Jenniskens et al. 2012; Borovička et al. 2021; McMullan et al. 2024). In any case, these fragile meteoroids often generate extremely bright bolides without yielding noticeable meteorites (Borovička et al. 2022). Over more than 25 years of operation, our SPMN network has recorded several cometary superbolides; one of the most memorable events occurred on July 11, 2008, which, due

to its anomalous orbit, was tentatively associated with the disruption of comet C/1919 Q2 Metcalf. (Trigo-Rodríguez et al. 2009).

In addition to the physical properties of SPMN180524F, its short perihelion distance suggests a relatively recent formation of the meteoroid. The inferred bulk density is consistent with that expected for a crumbly carbonaceous chondrite. It is well-known that common cometary outgassing cannot release meter-sized meteoroids, indicating that this meteoroid may be a remnant of a relatively recent disruption of its parent comet under the thermal stress imposed by the solar heat near its close perihelion (Jenniskens 2006; Jewitt 2008; Trigo-Rodríguez & Blum 2022).

Efforts have been made to estimate the uncertainties of the CNEOS catalog based on ground-based observations, revealing two groups of measurements: one with sufficient accuracy to allow acceptable heliocentric orbits, and another with significant radiant and velocity deviations Devillepoix et al. (2019) reported discrepancies in the radiants of CNEOS fireballs, ranging from a few degrees to as much as 90° . For example, velocity vectors were inaccurately measured for events such as Buzzard Coulee, 2008 TC3, Kalabity, and Crawford Bay. Specific typographical errors, like the missing minus sign in the z velocity component for 2008 TC3, were noted by Peña-Asensio et al. (2022), in addition to comparing two new events independently measured (2019 MO and 2022 EB5). Further independent analyses have included events like Saricicek, Ozerki, Viñales, Flensburg, Novo Mesto, and Adalen, which helped refine the mean radiant and velocity deviations of CNEOS fireballs (Brown & Borovička 2023; Peña-Asensio et al. 2024).

The superbolide SPMN180524F belongs to the group of events well-measured from space, as the apparent radiant is deviated in 0.98° and the velocity at the energy peak in 1.23 km s^{-1} , resulting in a relatively good agreement on the heliocentric orbit. This difference in velocity leads to a 0.71 au dissent in the semi-major axis. One notable divergence is the 4.43° of disagreement in slope, which yields a -2.81° discrepancy in the orbital inclination. It is worth noting the difference of -288 kg m^{-3} in density, mainly due to the 3.61 km of disagreement in the height where the radiation peak occurs.

4 CONCLUSIONS

The 18 May 2024 superbolide was a unique event that showcased how a fragile meter-sized meteoroid can produce a spectacular display of color and luminosity, and it exemplified how the Earth's atmosphere is an excellent shield for this type of impactor. A detailed analysis of the superbolide characteristics suggests that the meteoroid likely originated from the disruption of an eccentric comet, potentially explaining its relatively unstable orbit crossing the orbit of Jupiter. In any case, its short perihelion distance also suggests a recent detachment from its parent comet, as the long-term survival of fragile materials would be challenging under such thermal stress conditions close to the Sun. Given the high velocity and fragmentation observed, a meteorite's survival seems unlikely. However, the previous Maribo carbonaceous chondrite fall demonstrated that even weak meteoroids can produce small meteorites at relatively high speeds (Borovička et al. 2019).

Our analysis demonstrated relatively good agreement with the data reported by CNEOS both in radiant and velocity, and subsequently in the heliocentric orbital elements. We reconciled the satellite radiometric data with a purely dynamic atmospheric flight model to constrain the meteoroid's mass and consistently derive the atmospheric deceleration curve.

From an impact risk perspective, the event raises questions about

why a meter-sized meteoroid was not detected by current telescopic surveys, especially considering that these small object monitoring programs have successfully identified some asteroids of just a few meters in diameter before their collision with Earth. Our results provide a clear explanation: the meteoroid was simply too small and exhibited a low albedo to be detectable.

ACKNOWLEDGEMENTS

EP-A acknowledges support from the LUMIO project funded by the Agenzia Spaziale Italiana. JMT-R and PG-T acknowledge financial support from the Spanish project PID2021-128062NB-I00 funded by MCIN/AEI/10.13039/501100011033. PG-T acknowledges the financial support from the Spanish MCIU through the FPI predoctoral fellowship PRE2022-104624. We also acknowledge the monitoring effort made by the members of the SPMN Network. In particular, Miguel A. Furones, Miguel A. Garcia, and Antonio J. Robles, contributed to the SPMN recordings analyzed in this work. This work is partly based on data from AMS82 cameras of the AllSky7 network, and the authors thank the network operators, especially Juan Carlos Martín, for providing the data.

DATA AVAILABILITY

The data underlying this article will be shared on reasonable request to the corresponding author.

REFERENCES

- Borovička J., Popova O., Spurný P., 2019, *Meteoritics & Planetary Science*, **54**, 1024
- Borovička J., Bettonvil F., Baumgarten G., Strunk J., Hankey M., Spurný P., Heinlein D., 2021, *Meteoritics & planetary science*, **56**, 425
- Borovička J., et al., 2022, *A&A*, **667**, A157
- Bronshen V. A., 1983, *Physics of Meteoric Phenomena*. D. Reidel Publishing Company
- Brown P. G., Borovička J., 2023, *ApJ*, **953**, 167
- Brown P. G., et al., 2000, *Science*, **290**, 320
- Brown P., Spalding R. E., ReVelle D. O., Tagliaferri E., Worden S. P., 2002, *Nature*, **420**, 294
- Cepplecha Z., Borovička J., Elford W. G., Revelle D. O., Hawkes R. L., Porubčan V., Šimek M., 1998, *Space Science Reviews*, **84**, 327
- Cepplecha Z., Spalding E. R., Jacobs C., Revelle D. O., Tagliaferri E., Brown P., 1999, in Baggaley W. J., Porubčan V., eds, *Meteoroids 1998*. p. 37
- Collins G. S., Melosh H. J., Marcus R. A., 2005, *Meteoritics & planetary science*, **40**, 817
- Devillepoix H. A. R., et al., 2019, *MNRAS*, **483**, 5166
- Fulle M., Blum J., Rotundi A., Gundlach B., Güttler C., Zakharov V., 2020, *MNRAS*, **493**, 4039
- Gritsevich M. I., 2007, *Solar System Research*, **41**, 509
- Gritsevich M. I., 2009, *Advances in Space Research*, **44**, 323
- Haack H., et al., 2012, *Meteoritics & planetary science*, **47**, 30
- Jenniskens P., 2006, *Meteor Showers and their Parent Comets*. Cambridge University Press
- Jenniskens P., et al., 2012, *Science*, **338**, 1583
- Jewitt D., 2008, in , Saas-Fee Advanced Course 35: Trans-Neptunian Objects and Comets. p. 132
- Koschny D., Borovička J., 2017, WGN, Journal of the International Meteor Organization, **45**, 91
- Koschny D., et al., 2019, *Space Sci. Rev.*, **215**, 34
- Lauretta D. S., et al., 2024, *arXiv*
- McMullan S., et al., 2024, *Meteoritics & planetary science*, **59**, 927

- Moreno-Ibáñez M., Gritsevich M., Trigo-Rodríguez J. M., 2015, *Icarus*, **250**, 544
- Peña-Asensio E., Trigo-Rodríguez J. M., Langbroek M., Rimola A., Robles A. J., 2021a, *Astrodynamics*, **5**, 347
- Peña-Asensio E., Trigo-Rodríguez J. M., Gritsevich M., Rimola A., 2021b, *MNRAS*, **504**, 4829
- Peña-Asensio E., Trigo-Rodríguez J. M., Rimola A., 2022, *AJ*, **164**, 76
- Peña-Asensio E., Trigo-Rodríguez J. M., Grèbol-Tomàs P., Regordosa-Avellana D., Rimola A., 2023a, *Planet. Space Sci.*, **238**, 105802
- Peña-Asensio E., Trigo-Rodríguez J. M., Rimola A., Corretgé-Gilart M., Koschny D., 2023b, *MNRAS*, **520**, 5173
- Peña-Asensio E., Visuri J., Trigo-Rodríguez J. M., Socas-Navarro H., Gritsevich M., Siljama M., Rimola A., 2024, *Icarus*, **408**, 115844
- Peña-Asensio E., Sánchez-Lozano J. M., 2024, *Advances in Space Research*
- Revelle D. O., 2002, in Warmbein B., ed., ESA Special Publication Vol. 500, Asteroids, Comets, and Meteors: ACM 2002. pp 233–236
- Schräpler R. R., Landeck W. A., Blum J., 2022, *MNRAS*, **509**, 5641
- Silber E. A., Boslough M., Hocking W. K., Gritsevich M., Whitaker R. W., 2018, *Advances in Space Research*, **62**, 489
- Tagliaferri E., Spalding R., Jacobs C., Worden S. P., Erlich A., 1994, in Hazards Due to Comets and Asteroids. p. 199
- Tanbakouei S., Trigo-Rodríguez J. M., Blum J., Williams I., Llorca J., 2020, *A&A*, **641**, A58
- Trigo-Rodríguez J. M., 2022, Asteroid Impact Risk. Springer Nature
- Trigo-Rodríguez J. M., Blum J., 2022, *MNRAS*, **512**, 2277
- Trigo-Rodríguez J. M., et al., 2004, *Earth Moon and Planets*, **95**, 553
- Trigo-Rodríguez J. M., Madiedo J. M., Williams I. P., Castro-Tirado A. J., Llorca J., Vitek S., Jelínek M., 2009, *MNRAS*, **394**, 569
- Trigo-Rodríguez J. M., et al., 2014, *MNRAS*, **437**, 227
- Trigo-Rodríguez J. M., Rimola A., Tanbakouei S., Soto V. C., Lee M., 2019, *Space Sci. Rev.*, **215**, 18

This paper has been typeset from a $\text{\TeX}/\text{\LaTeX}$ file prepared by the author.